EVS26
Los Angeles, California, May 6-9, 2012

Visualization of Liquid Water Distribution in Fuel Cell by Using Neutron Radiography

Shintaro Tanaka, Yukihito Tanaka
Honda R&D Co., Ltd. Automobile R&D Center, Haga-gun, Tochigi, 321-3393 Japan,
Shintaro_Tanaka@n.t.rd.honda.co.jp
Yukihito_Tanaka@n.t.rd.honda.co.jp

Abstract

The accumulation of liquid water in the cell is given as a major factor affecting the electric generation performance of fuel cells, and the visualization and quantification of this liquid water is a key technology for fuel cell water management.

This study used neutron radiography to visualize the liquid water distribution inside a fuel cell during electric generation, and quantified the liquid water.

The results showed that resistance overpotential, which is one factor that reduces electric generation performance, tends to drop as the quantity of liquid water in the catalyst coated membrane increases. However, the resistance overpotential becomes constant at a certain quantity of liquid water or more. In addition, it was also shown that the amount of voltage drop during constant-load electric generation is strongly correlated with the quantity of liquid water in the cathode gas diffusion layer, and that the amount of voltage drop increases as the quantity of liquid water in the cathode gas diffusion layer increases.

This showed that higher electric generation performance can be obtained by changing the characteristics of the polymer electrolyte membrane and gas diffusion layer materials to increase the quantity of liquid water in the polymer electrolyte membrane, which requires water to manifest proper functions, while at the same time suppressing the quantity of liquid water in the gas diffusion layer, which has reduced functionality when water is present.

Keywords: fuel cell, PEM fuel cell (proton exchange membrane), ZEV (zero emission vehicle)

1 Introduction

Honda is developing fuel cell electric vehicles as a vital technology capable of addressing current issues facing mobility, including environmental issues such as global warming and air pollution, and energy issues due to depleting petroleum resources.

Fuel cells generate electric power by reacting the hydrogen supplied as fuel from the anode side with the oxygen in the air supplied from the cathode side. The reaction formulae for each side are as follows:

Anode (An): $H_2 \rightarrow 2H^+ + 2e^-$
Cathode (Ca): $1/2\ O_2 + 2H^+ + 2e^- \rightarrow H_2O$

Figure 1 shows the sectional structure of a fuel cell. The fuel cell reaction is performed by a membrane electrode assembly (MEA) obtained by joining a catalyst-coated membrane (CCM) created by attaching catalyst layers to both sides of a polymer electrolyte membrane (PEM), with gas diffusion layers (GDL). Inside the MEA, the PEM is a proton conductor that manifests proton conduction functions in the water retaining state, which is thought to lower the resistance overpotential that is one factor reducing electric generation performance. Conversely, liquid water accumulation in the GDL would lower the gas diffusivity of the GDL and reduce the oxygen concentration around the catalyst layers, which is thought to be one factor reducing electric generation performance. In this manner, the presence of water inside the MEA enhances the functions of some parts, while reducing the functions of other parts. Various studies [1]-[3] have been conducted on the relationships between the different functions and the quantity of water. However, so far no known studies have shown how the water distribution for the entire MEA should be modified to obtain even higher electric generation performance.

Neutron radiography was used to visualize the quantity of liquid water in each part of the MEA, and the relationship between this liquid water distribution and the resistance overpotential and the voltage drop during constant-load electric generation was investigated. These results were then used to clarify the relationship between the PEM and GDL characteristics and the liquid water distribution inside the MEA, and to investigate the enhancement of fuel cell electric generation characteristics.

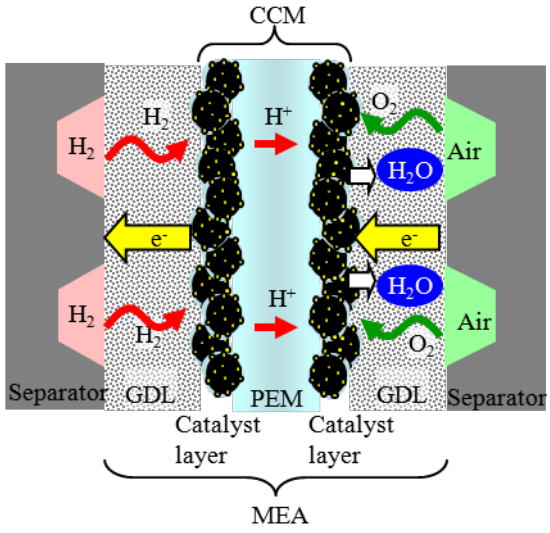

Figure 1. Schematic of fuel cell.

2 Experimental

2.1 MEA and Cell Configuration

Table 1 shows the tested MEA configurations. MEA-B used a GDL with increased gas diffusivity compared to the standard MEA-A, and MEA-C used a PEM with increased proton conductivity and water vapor permeability compared to MEA-B. The An and Ca catalyst layers used in each MEA were the same.

Figure 2 shows the cell configuration. The cell for neutron radiography was created by clasping an MEA consisting of a CCM and GDL, together with gaskets to prevent gas leakage, between two separators.

Table 1. MEA configurations

	PEM	GDL
MEA-A	Standard PEM	Standard GDL
MEA-B	Standard PEM	High gas diffusivity GDL
MEA-C	High proton conductivity and high water vapor permeability PEM	High gas diffusivity GDL

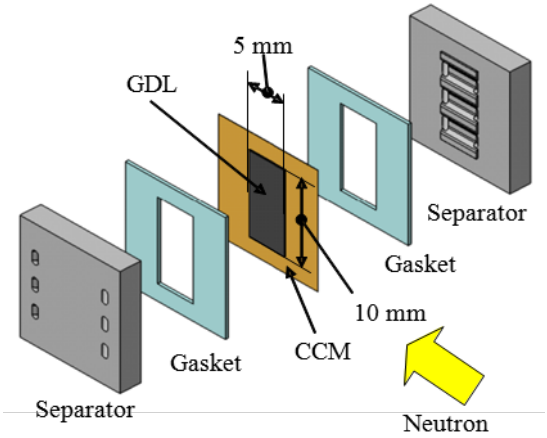

Figure 2. Configuration of cell for neutron radiography.

2.2 Neutron Radiography

Neutron radiography is a method enabling the quantification of substances using the neutron attenuation characteristics of the constituent atoms of the subject. Al, C, F and other elements often present in the component materials of fuel cells have small attenuation characteristics, but substances containing H atoms have large attenuation characteristics. These characteristics were used to measure the neutron attenuation of liquid water, which has a high concentration of H

atoms, and to visualize and quantify the liquid water in the cell section.
Figure 3 shows the mass attenuation coefficients of typical atoms and molecules with respect to thermal neutrons [4].

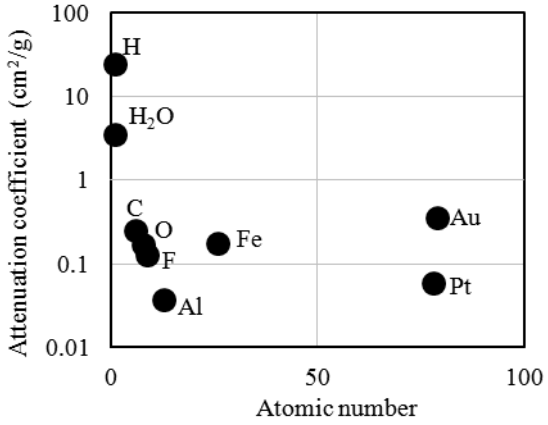

Figure 3. Attenuation coefficient of elements.

This shows that H_2O molecules, which include H atoms, have a larger mass attenuation coefficient compared to other atoms. (Note that H_2O is plotted according to the atomic number of H.) The Lambert-Beer law indicated by equation (1) is used to deduce the thickness t of the test piece from the neutron attenuation.

$$I_{out} = I_{in} \exp(-\alpha \cdot t) \quad (1)$$

Here, I_{in} is the incident neutron intensity, I_{out} is the transmitted neutron intensity, and α indicates the neutron mass attenuation coefficient of the test piece. The thickness of the liquid water in the MEA was measured as described above under various electric generation conditions. The liquid water in the MEA was then quantified by dividing the liquid water thickness by the thickness in the neutron ray direction of the effective electrode (described hereafter), and expressing the result as the liquid water occupancy per unit volume.
Neutron radiography measurements were performed at the ICON beam line of the Paul Scherrer Institute (PSI) in Switzerland, in collaboration with the PSI Electrochemistry Laboratory (ECL) and Neutron Imaging and Activation Group (NIAG). These measurements were based on the recent advances in high-resolution imaging of fuel cells realized at PSI [5], [6].

The neutron transmission image was measured from the cell section direction as shown in Figure 2. To increase the spatial resolution in the section direction in the observation region where the total of the flow field depths (An, Ca) and the MEA thickness is between 1 mm and 2 mm, measurement was performed by inclining the detector (CCD) relative to the section direction as shown in Figure 4 [5].

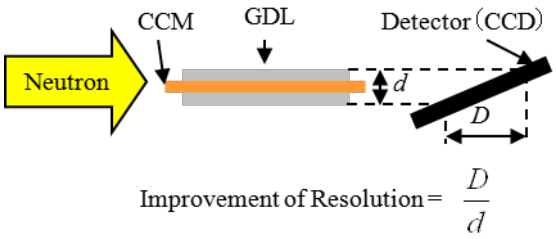

Figure 4. Schematic of increase in resolution.

By measuring with only one direction (in this study, the MEA thickness direction) of the neutron transmission image stretched in this manner, the resolution of the obtained image was increased from 13.5μm/pixel to 2.3μm/pixel. However, due to the limited collimation of the neutron beam and the inherent blurring of the detector, the actual spatial resolution was approximately 20μm.

2.3 Fuel Cell Operation

Electric generation was performed using MEA-A with the test conditions listed in Table 2 in order to clarify the relationship between the liquid water distribution in the MEA and overpotential. Electric generation was performed while varying the three parameters of the cell temperature, Ca gas humidity and An gas humidity. The terminal voltage and resistance overpotential during electric generation were measured, and the liquid water distribution in the MEA at that time was also visualized simultaneously.

Table 2. Test conditions for MEA-A.

Current density	1.0 A/cm^2
Cell temperature	50, 70, 85 deg. C
An gas	H_2
Ca gas	Air
An gas humidity	50～100 %RH
Ca gas humidity	40～100 %RH

Next, electric generation was performed using MEA-A, MEA-B and MEA-C under the test conditions listed in Table 3, and neutron visualization was performed to clarify the change in the liquid water distribution in the MEA due to different PEM and GDL.

Table 3. Test conditions for MEA-A, B, C.

Current density	1.0 A/cm^2
Cell temperature	70 deg. C
An gas	H_2
Ca gas	Air
An gas humidity	35～100 %RH
Ca gas humidity	35～100 %RH

3 Results and Discussion

3.1 Relationship between Change in Liquid Water Distribution in the MEA due to Electric Generation Environment, and Overpotential

Figure 5 shows examples of images obtained by neutron radiography of the liquid water distribution in MEA-A during electric generation. The blue-colored portions indicate liquid water. Electric generation was performed with a fixed current density of 1.0 A/cm^2, so the quantity of water generated by the fuel cell reaction was the same for any electric generation condition. However, when low-humidity gas was flowed to both electrodes as shown in Figure 5(a), the inside of the MEA was drier and there was less liquid water compared to when high-humidity gas is flowed as shown in Figure 5(b). (The cell temperature was 70°C in either case.)

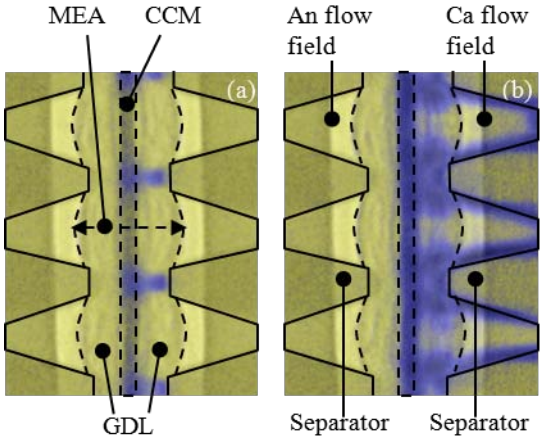

(a) An gas: 50 %RH
Ca gas: 40 %RH

(b) An gas: 100 %RH
Ca gas: 100 %RH

Figure 5. Images of liquid water distribution during electric generation and regions of quantitative analysis.

3.1.1 Relationship between Quantity of Liquid Water in the CCM and Resistance Overpotential

Figure 6 shows the resistance overpotential of MEA-A measured under each electric generation condition listed in Table 2.

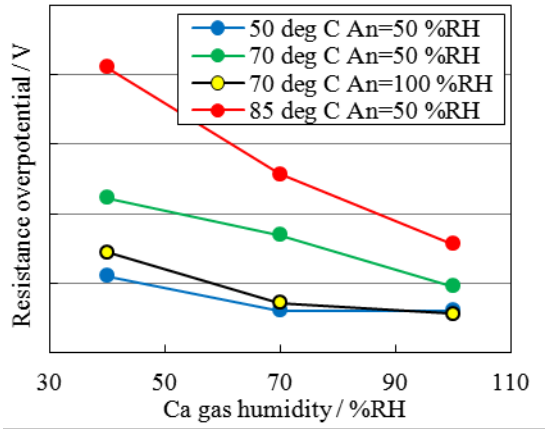

Figure 6. Resistance overpotential of each test condition.

At all cell temperatures, lowering the Ca gas humidity increased the resistance overpotential. In particular, at a cell temperature of 85°C that results in a high water saturation pressure, the increase in resistance overpotential as the Ca gas humidity decreased was larger than that at other cell temperatures. The quantity of liquid water measured using neutron radiography was compared to verify the relationship between the resistance overpotential and the quantity of liquid water in the MEA at this time. The factor influencing the resistance overpotential is thought to be the quantity of water in the PEM, so the ideal approach is to quantify only the liquid water in the PEM. However, the PEM thickness is relatively small given the neutron radiography resolution, and it is a challenge to clearly separate the quantities of liquid water in the PEM and the catalyst layers. Therefore, this study used the quantity of liquid water in the CCM. Figure 7 shows the relationship between the resistance overpotential and the quantity of liquid water in the CCM.

The resistance overpotential dropped as the quantity of liquid water in the CCM increased, but then became constant at a certain quantity of liquid water or more. This indicates that in order to increase electric generation performance, a certain quantity of liquid water or more should be maintained for the PEM to exhibit sufficient proton conduction functions.

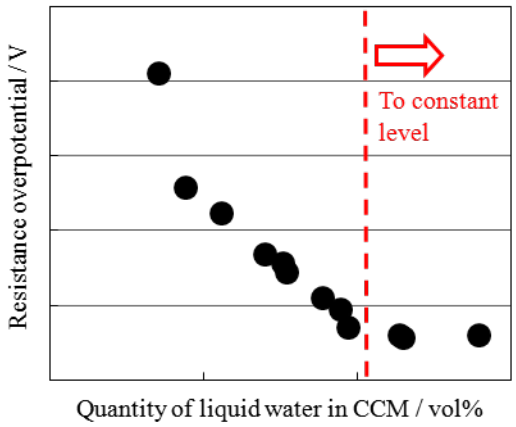

Figure 7. Relation between resistance overpotential and liquid water in CCM.

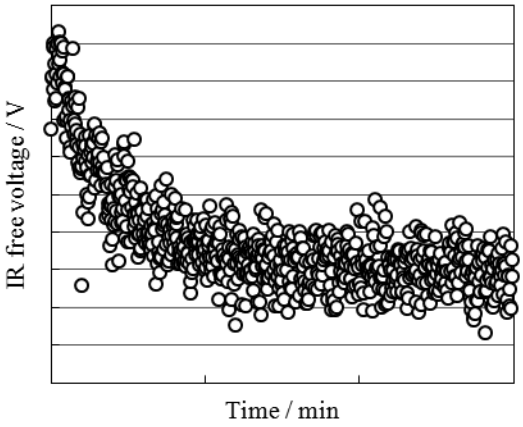

Figure 8. Time evolution of IR free voltage and voltage drop.

3.1.2 Relationship between Quantity of Liquid Water in the Ca GDL and Voltage Drop

There are two possible factors affecting the voltage drop during constant-load electric generation due to accumulation of liquid water in the MEA. One is a drop in gas diffusivity within the catalyst layer due to liquid water accumulating in the catalyst layer, and the other is a drop in the amount of gas movement to the catalyst layer due to liquid water accumulating in the GDL. Accurate measurement of the quantity of liquid water in the catalyst layer is a challenge because the catalyst layer thickness is relatively small given the neutron radiography resolution. Therefore, the relationship between the liquid water accumulated in the GDL and the voltage drop was verified using MEA-A. The voltage drop behavior was quantified by measuring the amount of voltage drop from the start of constant-load electric generation at 1.0 A/cm2. The terminal voltage includes the aforementioned change in resistance overpotential, so the drop in IR free voltage (sum of the terminal voltage and the resistance overpotential) that cancels out this change was used as the amount of voltage drop. Figure 8 shows an example of the IR free voltage behavior when electric generation is performed with a cell temperature of 50°C, An gas humidity of 50% RH and Ca gas humidity of 70% RH. Figure 9 shows the neutron visualization results measured at the same time (0 min and 10 min after the start of electric generation).

Figure 8 shows a high IR free voltage immediately after the start of electric generation, and Figure 9(a) shows that almost no liquid water has accumulated in the MEA at this time.

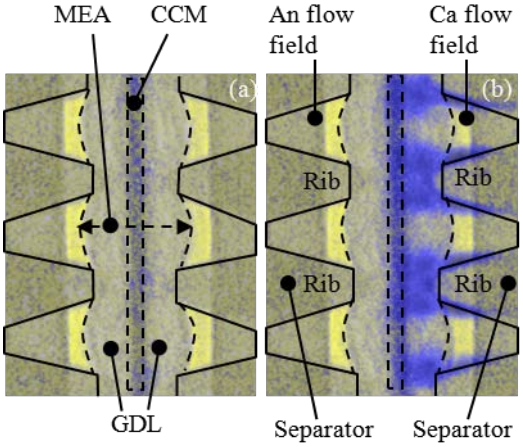

Figure 9. Change in liquid water distribution during electric generation (a) t = 0 min, (b) t = 10 min.

However, as constant-load electric generation continues, the IR free voltage drops to a constant value. Figure 9(b) shows that liquid water accumulates in the MEA by the time this IR free voltage constant region is reached, and that most of this liquid water accumulates in the Ca GDL near the Ca separator ribs.

Next, Figure 10 shows the amount of voltage drop during constant-load (1.0 A/cm^2) electric generation using MEA-A under each electric generation condition listed in Table 2.

The increase in the voltage drop amount due to changes in the Ca gas humidity is larger for a cell temperature of 50°C, at which there is low water saturation pressure, than at other cell temperatures. The quantities of liquid water in the Ca GDL measured by neutron radiography were compared to verify the relationship between the amount of voltage drop and the quantity of liquid water in the Ca GDL. As shown in Figure 9(b), the quantity of liquid water in the Ca GDL differs greatly near the gas flow fields and near the ribs (the convex

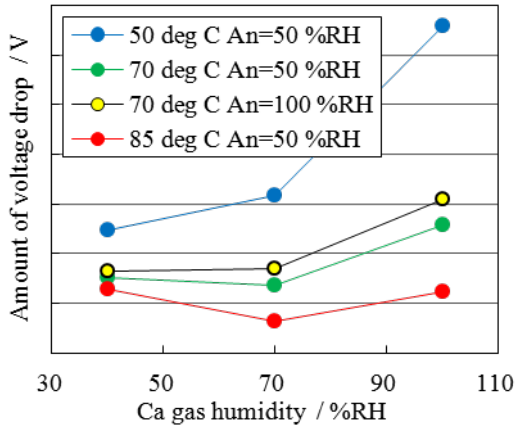

Figure 10. Voltage drop of each test condition.

portions of the separator that contact the Ca GDL for electric conduction), with more liquid water tending to be distributed near the ribs. This is thought to be because gas did not easily diffuse in the Ca GDL near the ribs, so there was less drying of the generated water compared to the flow fields. Therefore, the quantity of liquid water in the Ca GDL was measured for the three patterns of near the ribs, near the flow fields, and the average of the two (Ca GDL average), and the correlation between each pattern and the amount of IR free voltage drop was verified. The results for all patterns showed that when the quantity of liquid water in the Ca GDL increases, the amount of voltage drop also tends to increase. This confirmed that in order to suppress the voltage drop during constant-load electric generation, it is necessary to reduce the quantity of liquid water in the Ca GDL. Of the three patterns used to measure the quantity of liquid water, the Ca GDL average was most strongly correlated with the amount of voltage drop. Figure 11 shows the relationship between the average quantity of liquid water in the Ca GDL and the amount of voltage drop.

The reason for the strong correlation between the average quantity of liquid water in the Ca GDL and the amount of voltage drop is thought to be that the accumulation of liquid water reduces the Ca GDL gas diffusivity, which affects the gas movement. This behavior, where the movement of gas to the catalyst layers is impeded, is thought to be most closely represented by the average quantity of liquid water in the Ca GDL.

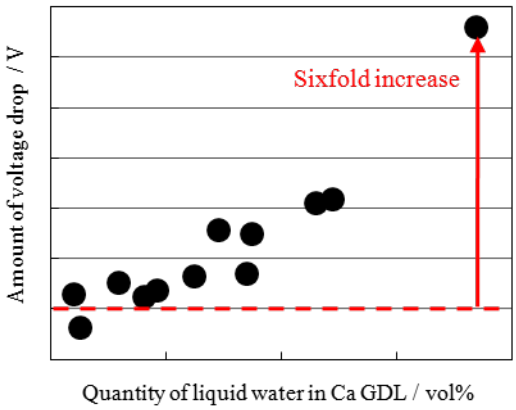

Figure 11. Relation between voltage drop and liquid water in Ca GDL.

3.1.3 Change in Liquid Water Distribution in the MEA due to Electric Generation Environment

Figure 12 shows the results of combining the relationship between the quantity of liquid water in the CCM and the resistance overpotential shown in Figure 7, and the relationship between the quantity of liquid water in the Ca GDL and the voltage drop shown in Figure 11. Note that the quantity of liquid water in the CCM is expressed as a percentage of the quantity of liquid water at which the resistance overpotential becomes constant as shown in Figure 7.

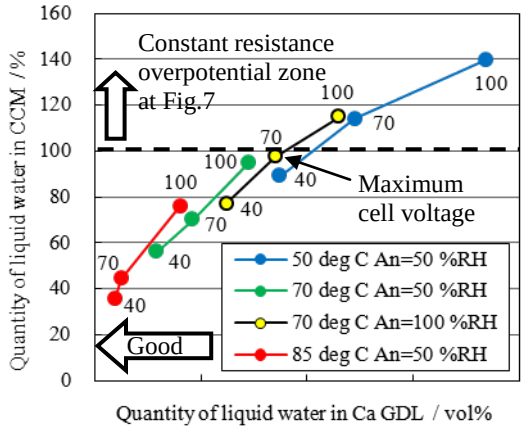

Figure 12. Relation between liquid water in CCM and Ca GDL (represented by cathode gas humidity).

Of the various test conditions used in this study, the maximum terminal voltage was obtained at a cell temperature of 70°C, An gas humidity of 100% RH, and Ca gas humidity of 70% RH. Figure 13 shows the neutron visualization image under these conditions, and indicates that these conditions result in the minimum quantity of liquid water in the CCM needed to reduce the resistance

overpotential to a constant value as shown in Figure 12. When drier conditions are used, the PEM cannot retain sufficient liquid water, which increases the resistance overpotential. When wetter conditions are used, the quantity of liquid water in the Ca GDL increases, which impedes the movement of gas to the catalyst layer. Both of these cases are thought to result in lower performance.

When considering the ideal water distribution in the MEA, it is thought important to retain a sufficient quantity of liquid water in the CCM (PEM) to manifest proton conduction functions, while at the same time minimizing the quantity of liquid water in the Ca GDL that impedes the movement of gas to the catalyst layer. However, when the cell temperature, gas humidity or other electric generation conditions are simply changed, the quantity of liquid water in the CA GDL increases together with that in the CCM.

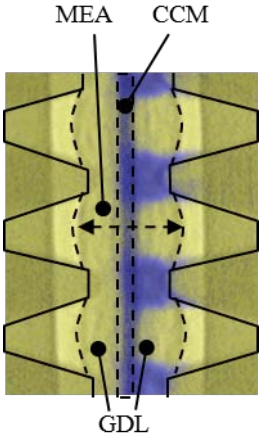

Figure 13. Image of liquid water distribution under the best condition of MEA-A
(An gas:100 %RH, Ca gas:70 %RH)

3.2 Change in Liquid Water Distribution in the MEA due to Different PEM and GDL

To enhance electric generation performance, it is considered necessary to develop materials, optimize layer structures, and investigate flow field structures in order to approach the ideal water distribution in the MEA. The changes in the water distribution in the MEA due to changing the PEM and GDL are described below.

3.2.1 Relationship between Change in Quantity of Liquid Water in the CCM due to Different PEM, and Resistance Overpotential

Figure 14 shows the resistance overpotential of MEA-A, MEA-B and MEA-C measured under each electric generation condition listed in Table 3.

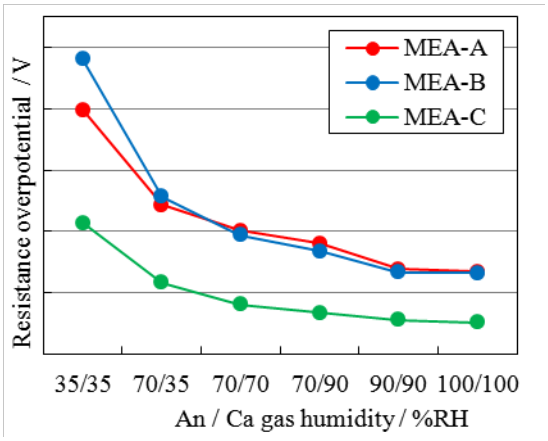

Figure 14. Resistance overpotential in several humidity conditions.

MEA-C, which used a PEM with higher proton conductivity than the PEM used in MEA-A and MEA-B, exhibited a lower resistance overpotential value than that of MEA-A and MEA-B over the entire tested humidified condition range. Next, Figure 15 shows the relationship between the quantity of liquid water in the CCM obtained by neutron radiography, and the resistance overpotential.

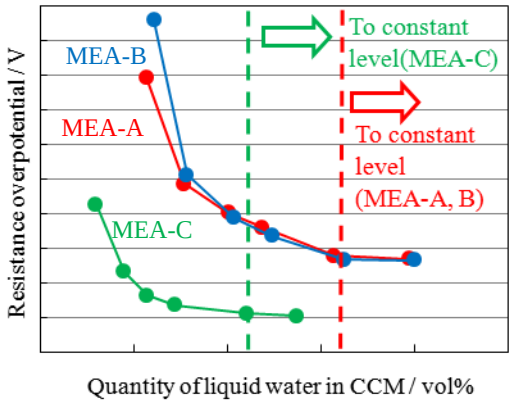

Figure 15. Relation between resistance overpotential and liquid water in CCM.

This shows that the PEM used in MEA-C manifests higher proton conduction functions than the PEM used in MEA-A and MEA-B, even at the same quantity of liquid water. In addition, it also shows that the PEM used in MEA-C tends to reach a constant resistance overpotential at a lower

quantity of liquid water compared to the PEM used in MEA-A and MEA-B.

3.2.2 Change in Quantity of Liquid Water in the Ca GDL due to Different PEM and GDL

Figure 16 shows the results of using neutron radiography to measure the average quantity of liquid water in the Ca GDL under each electric generation condition listed in Table 3. In addition, Figure 17 shows examples of the liquid water distributions in MEA-A, MEA-B and MEA-C when electric generation is performed under the same electric generation conditions. The electric generation conditions used were An gas humidity of 90% RH and Ca gas humidity of 90% RH.

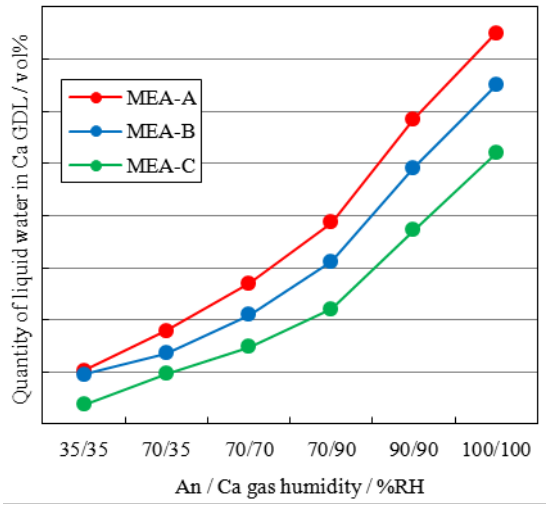

Figure 16. Quantity of liquid water in Ca GDL in several humidity conditions.

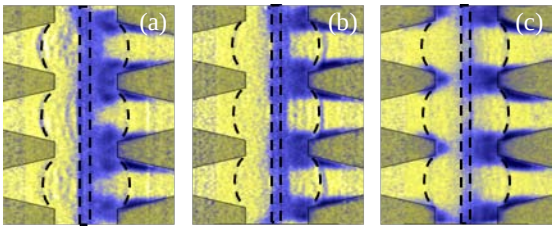

Figure 17. Images of liquid water distribution of MEA-A (a), MEA-B (b), MEA-C (c).

These results show that MEA-B had less liquid water in the Ca GDL, which is a factor resulting in voltage drop, compared to MEA-A. This is thought to be because MEA-B, which used a GDL with higher gas diffusivity, more easily discharged the water generated by the fuel cell reaction to the flow field side in the water vapor state, which suppressed the accumulation of liquid water in the Ca GDL. In addition, MEA-C had even less liquid water in the Ca GDL compared to MEA-B, which is thought to be because the liquid water accumulated near the An separator ribs. The reason for this is thought to be that the PEM with higher water vapor permeability experienced more water movement (back diffusion) via the PEM due to the difference in water vapor partial pressure between the An and Ca, which further suppressed the accumulation of liquid water in the Ca GDL.

3.2.3 Control of the Liquid Water Distribution during Electric Generation by Using Different PEM and GDL

Figure 18 shows the results of combining the results shown in Figure 12 and the quantities of liquid water in the CCM and GDL of MEA-A, MEA-B and MEA-C during electric generation, measured by the same method.

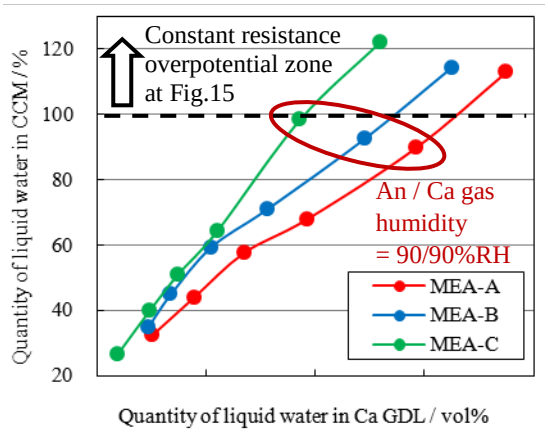

Figure 18. Relation between liquid water in CCM and Ca GDL.

Comparison of the quantity of liquid water in the Ca GDL at the same quantity of liquid water in the CCM shows that MEA-B suppressed the accumulation of liquid water in the Ca GDL compared to MEA-A. In addition, MEA-C, which used a PEM with higher water vapor permeability, further suppressed the accumulation of liquid water in the Ca GDL compared to MEA-B. It is thought that this was achieved due to the two effects of 1) lower relative humidity on the Ca side as a result of back diffusion due to water vapor permeating the PEM, and 2) the PEM used in MEA-C exhibiting proton conductivity at a lower quantity of liquid water compared to the PEM used in MEA-A and MEA-B.

These results confirmed that the distribution of liquid water in the MEA can be changed by changing the PEM and GDL characteristics in this manner, even when electric generation is performed under the same conditions. Figure 19

shows an example of the terminal voltage and resistance overpotential of MEA-A, MEA-B and MEA-C when electric generation is performed under the conditions of An gas humidity of 90% RH and Ca gas humidity of 90% RH indicated in Figure 18.

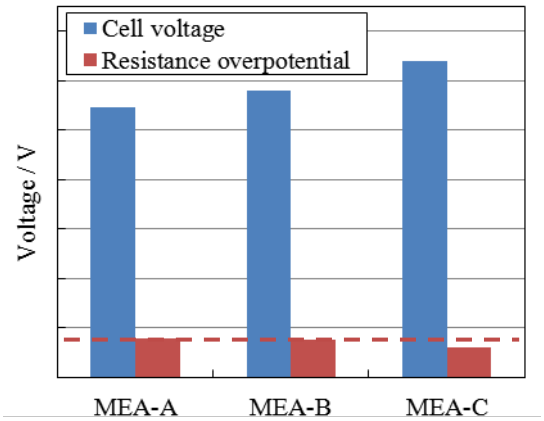

Figure 19. Cell voltage and resistance overpotential of each MEA (An / Ca Gas humidity = 90/90%RH).

MEA-A and MEA-B have the same resistance overpotential, but MEA-B exhibits a higher terminal voltage as a result of less liquid water accumulating in the Ca GDL due to use of a GDL with high gas diffusivity. In addition, MEA-C achieves a higher terminal voltage than MEA-B as a result of the two factors of reduced resistance overpotential due to use of a PEM with high proton conductivity and high water vapor permeability, and lower Ca relative humidity due to back diffusion of water vapor, which suppressed the accumulation of liquid water in the Ca GDL.

4 Conclusions

It was confirmed that a more ideal liquid water distribution, with less liquid water accumulating in the Ca GDL and the minimum liquid water content in the PEM needed to lower resistance, can be approached and higher electric generation performance can be obtained by changing the PEM and GDL.

(1) The resistance overpotential tends to drop as the quantity of liquid water in the CCM increases, but becomes constant at a certain quantity of liquid water or more.

(2) The amount of voltage drop increases after the start of constant-load electric generation as the quantity of liquid water in the Ca GDL increases.

(3) The accumulation of liquid water in the Ca GDL is suppressed and electric generation performance is enhanced by using a GDL with high gas diffusivity and a PEM with high water vapor permeability.

References

[1] P. Boillat, P. Oberholzer, R. Perego, R. Siegrist, A. Kaestner, E.H. Lehmann, G.G. Scherer, A. Wokaun: ECS Transactions, 41 (1) 27-38 (2011)

[2] J. S. Preston, U. Pasaogullari, D. S. Hussey, D.L. Jacobson: ECS Transactions, 41 (1) 319-328 (2011)

[3] J. M. LaManna, S. Chakraborty, F. Y. Zhang, J. J. Gagliardo, J. P. Owejan, M. M. Mench: ECS Transactions, 41 (1) 329-336 (2011)

[4] http://rrsys.tokai-sc.jaea.go.jp/rrsys/html/riyou_bunya/pdf/0607.pdf

[5] P. Boillat, G. Frei, E. H. Lehmann, G. G. Scherer, A. Wokaun.: Neutron Imaging Resolution Improvements Optimized for Fuel Cell Applications, Electrochem. Solid-State Lett. 13, B25 (2010)

[6] P. Boillat, G. G. Scherer: Chapter 12 of Neutron Radiography, edited by Wang, H., Yuan, X., Li, H.: Handbook of PEM fuel cell durability, Volume 2, PEM fuel cell diagnostics tools, Taylor & Francis Group, LLC, CRC, In Press (2011)J.J. Romm, *The hype about Hydrogen*, ISBN 1-55963-704-8, Washington, Island Press, 2005

Authors

SHINTARO TANAKA
Assistant Chief Engineer
Honda R&D Co., Ltd. Automobile R&D Center
4630 Shimotakanezawa, Haga-machi, Haga-gun, Tochigi, 321-3393 Japan
E-mail
Shintaro_Tanaka@n.t.rd.honda.co.jp

YUKIHITO TANAKA
Assistant Chief Engineer
Honda R&D Co., Ltd. Automobile R&D Center
4630 Shimotakanezawa, Haga-machi, Haga-gun, Tochigi, 321-3393 Japan
E-mail
Yukihito_Tanaka@n.t.rd.honda.co.jp